A Soft Robotic Exo-Sheath using Fabric EMG Sensing for Hand Rehabilitation and Assistance

Jiaqi Guo, Shuangyue Yu, Yanjun Li, Tzu-Hao Huang, Junlin Wang, Brian Lynn, Jeremy Fidock, Chien-Lung Shen, Dylan Edwards, and Hao Su*

Abstract— **This paper presents the design and evaluation of a soft robot exo-sheath for the hand that integrates a soft fabric electromyography (sEMG) sensor. The robot will utilize EMG signals to actuate movement and improve rehabilitation therapy and activities of daily living (ADL) in stroke and spinal cord injury (SCI) patients. This wearable robot addresses the limitations of previously developed soft robot gloves by improving ergonomics designs and clinical practice. A compact design makes the robot portable, with electric actuation that uniquely reduces shear forces and avoids kinematic singularity. Disparate from conventional robotic gloves, this design optimizes a bio-inspired fin-ray structure to enhance hand proprioception by leaving the palm uncovered. This glove incorporates novel self-fastening finger clasps and a soft fabric EMG sensor that allow wearers to self-don/doff the device and control movement, respectively. The functionality of this soft robot has been demonstrated with experimental results using low-level position control, kinematic evaluation, and reliable EMG measurements.**

I. Introduction

The human hand is one of the most complex products of evolution. Hand rehabilitation relies on neural plasticity, the underlying mechanism that drives motor recovery after stroke and spinal cord injury (SCI) [1]. Meanwhile, hand rehabilitation has been formidably challenging to accomplish due to the complexity of sensorimotor control required for hand function.

Wearable robotics research is going through several key paradigm shifts. There is a dichotomy in robot development. Some designs focus on creating movement about one or more joints, known as joint-space; others focus on generating movement around a task, known as task-space. The early pioneering works in this field typically fall into the second category. The task-space type robots assist the distal portion of the users (the end-effector using robotics terminology), such as MIT MANUS [2], the Mirror Image Movement Enabler (MIME) robotic device [3], and the Amadeo robotic system [4]. These typically have relatively simple mechanisms and less degrees of freedom (DOF) than joint-space type robots. The joint-space type robots are primarily developed for rehabilitation applications and typically fixed on a base platform and not wearable. These robots assist users in the anthropomorphic joint space providing natural movement, e.g. the upper limb exoskeletons by Kim et al. [5] for shoulder joint and Gijbels et al. [6] for the upper limbs. These are typically wearable robots that have articulated structures and the same DOF as their biological counterparts.

Another trend in rehabilitation robots is to shift from bulky and rigid designs to soft or hybrid rigid/soft designs. Compared with traditional rigid designs, soft robotics has demonstrated its potential due to comfortable human-robot interaction and ability to interact with unknown properties in its environment. Soft wearable robots typically consist of three key sub-systems: an actuation unit, transmission unit and a wearable unit.

In terms of actuation approaches, soft hand exoskeletons can be classified into two main categories: pneumatic and electrical actuations. Pneumatically actuated hand orthoses, represented by the Harvard soft robot glove Polygerinos et al. [7], [8] and the National University of Singapore pneumatic soft glove [9][10], are typically not portable, as each requires a cumbersome and bulky air pump. In terms of electrical actuation, Jeong et al. and Kang et al. employed a bio-inspired, soft, tendon-driven system called Exo-Glove Poly [11]–[15], that leverages silicone in its wearable structure to maintain hygiene and washability. Xiloyannis et al. [16] developed a tendon-driven robotic glove using Bowden cable transmission and a brushless motor actuator to under actuate 8 DOF. Researchers from the Bioservo Technologies AB [9], [17] designed a textile based soft extra muscle glove.

There is a strong unmet clinical need to develop hand orthoses that incorporate both robotics and clinical considerations to assist SCI, stroke, and elderly assistive populations [18][19][20]. First, a compact and portable design is desirable. Thus, wearers can use devices for both rehabilitation and assistance. Second, to enhance acceptance rates, it is crucial to optimize comfort. Tendon-driven hand orthoses typically suffer from kinematic singularity and apply significant shear forces. Third, to maintain the patient's proprioception and sensation, user's palms should be minimally covered [21]. Fourth, users prefer an exoskeleton that has self-dressing capability which does not require assistance from others.

Besides electromechanical requirements, an intuitive user interface that detects human intention can significantly simplify device operation. Prior studies have integrated electrodes into the apparel to measure human physiological signals, such as cardiopulmonary monitoring [22]–[24], ECG sensing by conductive yarn [22], [23], motion sensing by piezo-resistive yarn [25], [26] and electromyography (EMG) measurement [27]–[29]. This device is more comfortable than previous devices that use embroidery or woven EMGs due to its knitting-based electrode incorporation.

In order to meet electromechanical requirements combined with an intuitive user interface, a soft under-actuated hand exoskeleton integrated with a soft fabric sEMG interface [30], [31], as shown in Fig. 1. The system has two DOF on per finger (flexion and extension) and can be used for both rehabilitation and home-assistance purposes. Unlike the traditional pulley

Jiaqi Guo, Shuangyue Yu, Tzu-Hao Huang, Junlin Wang, Yanjun Li, Brian Lyn and Hao Su are with the Biomechatronics and Intelligent Robotics Lab, Department of Mechanical Engineering, City University of New York, City College, NY, USA. *Corresponding author: hao.su@ccny.cuny.edu

Chien-Lung Shen is with the Taiwan Textile Research Institute, Taiwan, Republic of China.

Jeremy Fidock and Dylan Edwards are with the Department of Neurology, Weill Cornell Medicine, Cornell University, NY, USA.

system used in most motor-actuated designs, a bio-inspired, fin-ray structure [30], [31] is adapted to reduce weight and size in transmission. Therefore, this structure achieves a portable, compact system with optimized force transmission which could reduce shear force on fingers and improve user experience.

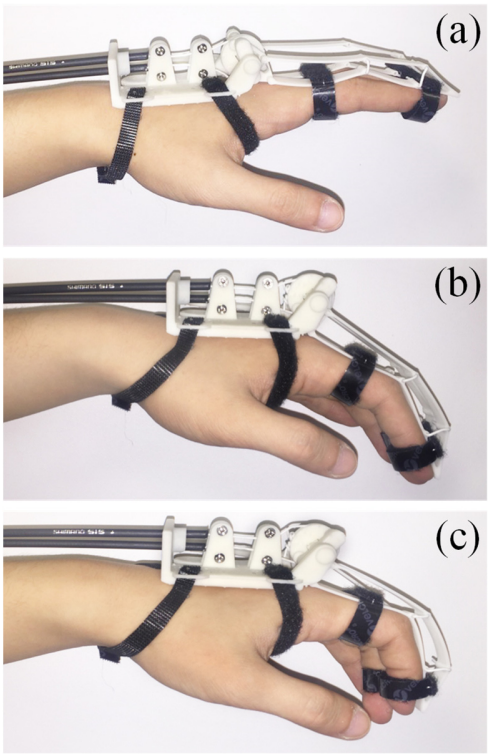

Fig. 1. Soft, bidirectional, tendon-driven hand exoskeleton is lightweight and assists both hand flexion and extension. It has the potential to be used for both stroke and SCI patients. (a) shows the hand extension posture with exoskeleton assistance to improve hand function of stroke patients. (b) is the neutral posture. (c) shows the hand flexion posture with exoskeleton assistance to improve hand function of SCI patients.

II. Design Requirements

In a nutshell, desire exists for a soft robotic exoskeleton that can reinstate hand strength in stroke and SCI patients. A traditional pulley system like the one used in the Exo-Glove Poly, and other cable-driven designs, bring huge amounts of shear force to patients' fingers, leading to an unpleasant user experience. Therefore, an adaptive fin-ray gripper structure [32], [33] was adjusted and applied to reduce shear force and achieve better transmission. Using this structure, one actuator can under actuate metacarpophalangeal (MCP), peripheral interphalangeal (PIP) and distal interphalangeal (DIP) joints in flexion and extension. A fabric sEMG interface was also explored and its output data was studied by a SVM classifier to detect and understand patients' intentions. Detailed design requirements of kinematics and kinetics parameters were assembled in Table 1.

A. Kinetic Requirements

The soft exo-glove is designed to help with both rehabilitation and activities of daily living (ADL). Thus, it is important to study patients' hand biomechanics to understand how much strength is needed to perform ADLs. The amount of strength that stroke or SCI patients use to voluntarily grip is often viewed as a measurement of hand function. According to previous research [9], [12], [15], [34], patients' grip strength shows great variance (18N ±27 N). The design requirement for force output therefore reflected the worst performers in these studies, patients with zero grip strength. This is intended to allow the robotic exo-glove to meet the demand of all patients in both rehabilitation and ADL scenarios.

A traditional bioinspired pulley structure has previously been explored to drive patients' fingers to perform flexion and extension [35]–[37]. In this structure, a cable is attached to the surface of fingers and pulls a knot above each finger to rotate around the joint accordingly. A major drawback of the traditional pulley system is that it applies a great amount of shear force to patients' fingers and results in an unpleasant user experience. An adaptive gripper structure was studied and adjusted to achieve an improved power transmission structure and provide better user comfort.

B. Kinematic Requirements

In rehabilitation procedures, patients are asked to perform various hand motions according to instructions from rehabilitation or medical devices [38]. Instead of accurate and powerful grasp of weighted objects, the initial phase of rehabilitation requires merely simple hand motions, such as flexion and extension of individual fingers. Therefore, force output strong enough to drive fingers is sufficient for rehabilitation procedures. As for activities of daily living, there are three main tasks that are performed several times every day by healthy people: typing with a keyboard, holding a bottle, and opening a door using a doorknob. The maximum values of range of motion (ROM) and force during these activities is another design criteria of the hand exoskeleton.

This paper explores the fin-ray structure as a medium of force transmission to fingers. However, unlike its implementation in the Festo Adaptive Gripper, the fin-ray structure must be adjusted to fit human hand curvature, as the initial states of human fingers of both healthy people and stroke or SCI patients are not straight. In this paper, curvature of seven hands from different people are studied to find an averaged initial state. Experimental objects are required to sit still and place their hands on a horizontal plane while keeping their hands relaxed. Further, they are required to hold bottles with normal force and lift them into the air. Pictures of their hands are captured in both relaxed and grasping states, and manually marked finger joints and phalanges in MATLAB MathWorks 2017b[9]. The data was used to generate kinematic parameters.

C. Intelligent System & Intention Detection Requirement

To help patients accomplish ADLs, the exo-glove system is required to have the ability to actively detect patients' intentions. In Nilsson's design [15] , pressure sensors are attached to each fingertip, and the system provides users with hand strength proportional to the feedback of the pressure sensors. In contrast, in Exo-Glove Poly [39] , an analog switch is the only input to control flexion and extension. In this paper, we propose a wearable sEMG interface that detects muscle signals from patients' arms. A SVM classifier interprets the data collected from the sEMG to understand patients' intentions.

TABLE I. COMPARISON OF DESIGN REQUIREMENT FOR REHABILITATION AND ASSISTANCE PURPOSES

Parameters	Rehabilitation	Assistance
Weight (g)	500	300
Actuated DOF	1	1
Size (mm^3)	154 × 40 × 14	154 × 40 × 14
Distal phalange ROM (deg)	+10 ~ -145	+5~ -100
Metacarpal ROM (deg)	+10 ~ -30	+5 ~ -45
Grip Force (N)	N/A	35
Intention Detection	N/A	sEMG

III. SYSTEM DESIGN

A detailed system design and construction procedures were developed to meet design requirements. The following sections describe each component in detail: actuation and transmission design, wearability design, electronics design, and sEMG interface design.

A. Actuation & Transmission Design

The entire mechanical transmission system is a combination of Bowden cables, pulleys and grippers (Fig. 2a). The flexible grippers maintain a tight fit and comfortable interaction with the fingers. This system also allows bidirectional and long-distance transmission of the assistive power to human fingers, so it is not necessary to mount the heavy electric motor near the fingers. As a result, the system on the back of the hand can be simple and light. The Bowden cable can remotely transfer the output power of the motor to the pulley fixed on the support pad (pulley1). Then, pulley1 further transfers the power to two fin-ray grippers with a shaft, driving the grippers to provide required forces and help patients extend or flex their index and middle fingers.

We select Faulhaber's DC motor 2232U012SR as the actuator of our system. Integrated with a gear reducer, the DC motor can generate torque up to 1Nm and maintains good backdrivability. The output shaft of the motor and the axle hole of a pulley (pulley2) form an interference fit, so the pulley can rotate together with the motor shaft and drive the cables.

The Bowden cable system includes cables, cable sheaths and cable mounts. This system can provide a steady bidirectional transmission process even when the hand is moving. With sheaths outside, Bowden cable can keep a constant length between cable mounts, so it will not become slack compared with no sheath condition. This characteristic gives Bowden cables the unique ability to transmit power with the movement of the hand. However, because of the stiffness, it is hard to loop the conventional steel Bowden cables over our small pullies. To solve this problem, we adopt thin Vectran lines to replace steel cables for receiving or outputting torque. To allow the cable system to transmit bidirectional forces, a pulley drives or is driven by two cables in our design. The ends of the two cables are put in the hole on the surface of the pulley groove, with two large knots to prevent themselves from escaping the hole. Regardless of the direction of the rotation, pulley2 will always pull one of the cables. Therefore, this design endows our cable system with the ability to apply bidirectional forces.

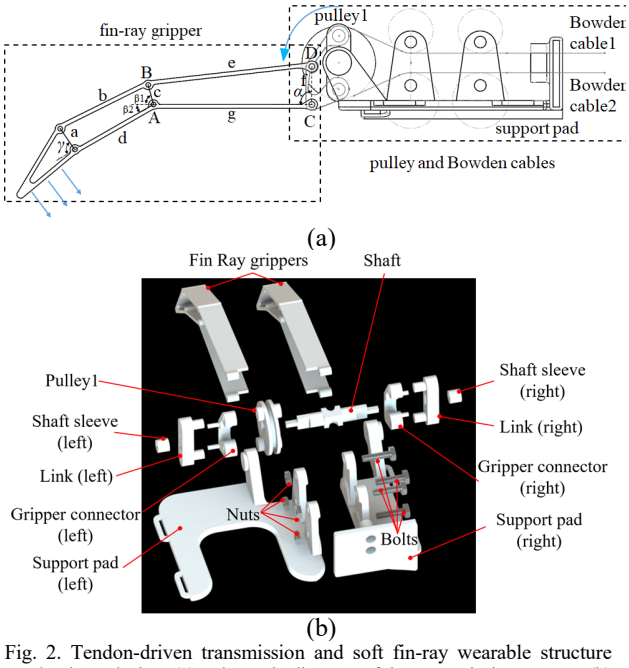

Fig. 2. Tendon-driven transmission and soft fin-ray wearable structure mechanisms design. (a) Schematic diagram of the transmission system. (b) Exploded view of components. The transmission system consists of bio-inspired fin-ray gripper, pulleys and Bowden cable system. The grippers are feasible and capable of fitting tightly with the fingers, while the shear force in the human-exoskeleton during pull and push can be kept in a reasonable level. The pulleys and Bowden cables can steadily transmit bidirectional torque to the gripper. All these components are mounted on a support pad with two parts connected by bolts and nuts. For simplification, the remotely mounted electric motor and the pulley2 connected with it are not shown in this figure.

Due to the versatility and the simplicity in designing and manufacturing, we employ pulley1, a shaft and two small links to apply torques on the two fin-ray grippers. This mechanism provides the grippers with a sufficient region of motion to help patients flex or extend their fingers, while the uncomfortable sliding motion and shear forces between the grippers and the fingers are kept to a low level. With the mate between the square hole of Pulley1 and the rectangular shaft, Pulley1 can drive the shaft without extra complex structures. Similarly, two small links with rectangular holes can rotate together with the shaft and drive the grippers to pull or push the fingers.

As described above, we use two cables to drive pulley1, which means pulley1 can rotate around half of a circle from the initial position (the initial position is the point where the system keeps the fin-ray grippers vertical). To reduce the sliding motion between the bottom surface of the fin-ray grippers and the upper surface of fingers, we adopt two design principles. The first principle is reducing the radius of pulley1, and the second is reducing the distance between the shaft and the fingers as much as possible. By keeping the center of rotation close to the fingers, such a design can largely eliminate the discomfort resulting from shear force. The components on the back of the hand are mounted on a stable support pad, whose bottom surface is designed to fit the dorsal surface of the hand, while the upper surface is flat. The support pad is fixed with the hand by four Hook and Loop fastening straps. Fig. 2 (b) shows the exploded view of these parts.

In this paper, we modified the fin-ray structure such that the shear force between fingers and grippers can be further reduced. The fin-ray effect, first discovered by Leif Kniese in

1997, describes a flexible structure that transmits forces. The fin-ray structure consists of two cartilaginous longitudinal rays that are attached to each other at either side and connected in the middle by separated elastic tissue. When forces are loaded on either side of the rays, the overall structure bends towards the direction of the load. The technical design in some researches like the Festo Adaptive Gripper is simple: an actuate-angled triangle with flexible sides stands as the basic element, and articulated braces are connected to both sides and keep them apart. When there is no load on the system, the two sides of the triangle remain straight. However, this initial state does not fit the curve of relaxed human hands. In our studies, we viewed the fin-ray structure as two connected four-bar linkage mechanisms to simplify kinematic analysis, and the layout of connective braces and the length of each side in the linkage are modified to fit human hand biomechanics.

With the simplification of the gripper to a linkage system, we analyzed the kinematics of the gripper. The entire transmission system has three degrees of freedom (DOF). Because the distance of AB is invariant during the motion, the constraint equation of the four-bar linkage ABCD is:

$$\left(\overrightarrow{CD}+\overrightarrow{DB}-\overrightarrow{CA}\right)\bullet\left(\overrightarrow{CD}+\overrightarrow{DB}-\overrightarrow{CA}\right)=c^2 \qquad (1)$$

After expanding Eq. (1), the relationship between α and β1 in Fig. 3 can be describe as:

$$2fgcos\alpha=2cgcos\beta_1-2cfcos(\beta_1-\alpha)+c^2-e^2+f^2+g^2 \qquad (2)$$

Similarly, γ can be determined once β1+β2 is known:

$$2adcos\gamma=2cdcos\left(\beta_1+\beta_2\right)-2accos(\beta_1+\beta_2-\gamma) +a^2-b^2+c^2+d^2 \qquad (3)$$

where a, b, c, d, e, f and g are the lengths of the links.

With 3D printing technology, we executed a rapid prototype development of our actuation system. This method allows us to design multi-functional parts with complex features, and manufacture or assemble them in a short time. The obtained parts are not only light, but also strong. Except for the cables, we printed all components in our actuation system by Form 2, a 3D Printer produced by Formlabs. It took about four hours to print these parts in Photopolymer Resin material.

B. Self-Fastening Finger Clasp

The design of the exo-glove necessitates a flexible mechanism to connect the transmission to the human hand. The patient must be able to mount the exo-glove with no assistance from another person, and fully flex his or her finger. The mechanism must be able to remain in place despite applied distal and proximal and transmit flexion and extension forces to the finger.

The design of the finger clasp is modeled after the medical finger trap used in closed fracture-reduction procedures. The interwoven mesh allows a finger to slide into the clasp with only a proximal force applied to the end (Fig. 3a, b). The mesh locks the finger in place when a distal force is applied to the clasp (Fig. 3c). The distal end of the finger clasp is capped to prevent proximal translation of the clasp. To release, a distal force is applied to the proximal end of the clasp.

The finger clasp is 3D printed using elastic thermoplastic polyurethane filament. This inexpensive material has a shore hardness of 85A, allows 660% maximum elongation, is chemical resistant, and does not dissolve in or absorb water. This method also allows each clasp to be fabricated to custom dimensions for the best fit.

The primary feature of the self-fastening finger clasp is the patient's ability to don and doff the device without assistance. Secondly, the clasp allows for flexion of the finger with no restriction. Thirdly, the clasp does not cover the palm, allowing the skin to breathe. Lastly, the clasp is inexpensive, robust, and versatile.

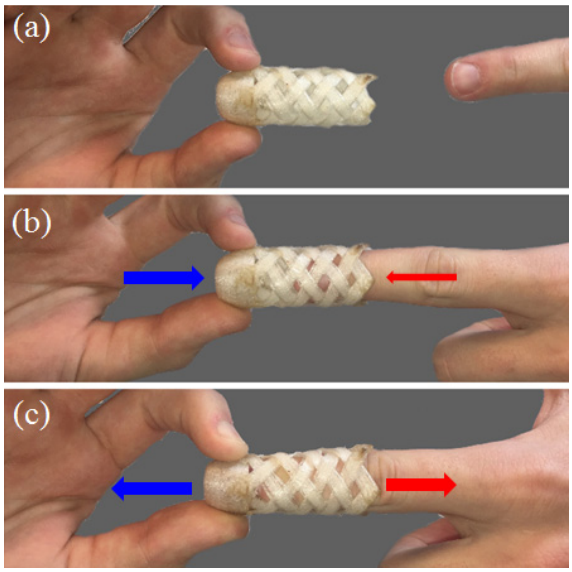

Fig. 3. Self-fastening finger clasp. (a) The initial status of finger clasp. (b) While putting on the clasp, assistive hand pushes the clasp to the finger. Blue arrow denotes the direction of force from the assistive hand, and red arrow denotes the friction from the finger. Notice the friction is relatively small because the mesh is loose. (c) If the clasp is pulled by the tip, denoted by the blue arrow, the mesh on the finger will be fastened, and thus generates a large opposite force, denoted by the red arrow, to hold the clasp on the finger.

C. Soft Fabric sEMG Sensor

A fabric-based soft wearable system that can be comfortably worn by users has been designed to detect sEMG signal (Fig. 4a). It can be used to detect patients' movement intention and help realize his/her finger's flexion or extension. The wearable sEMG detection system mainly consists of wearable electrodes and signal processing board.

For the measurement of the EMG signal, a silver knit fabric electrode with low resistance was designed. The property of the silver yarn is shown in Table II. The resistance of 10-centimetre interval of fabric electrode is tested, and there are three kinds of conditions for testing: 1. Measure the resistance of dry electrode directly; 2. Measure the resistance after putting fabric electrode into acid liquid 24 hours and placing in the shade to dry; 3. Measure the resistance after putting fabric electrode into alkali liquid 24 hours and placing in the shade to dry according to ISO105-E04. The results showed the maximum resistance is below 16.8Ω in all testing and the resistance was low enough for measuring the EMG signal.

TABLE II. THE RESISTANCE OF CONDUCT FABRIC AFTER ACID AND ALKALI PROCESSING, DEMONSTRAING ITS FEASIBILITY TO BE USED IN CONTACT WITH HUMAN SKIN WITH SIMILAR ACID AND ALKALI ENVIRONMENT

Processing Method	Resistance
Dry fabric	1.2±0.1Ω
Acid liquid	14.7±2.1Ω
Alkali liquid	6.5±0.8Ω

The textile EMG sensor was developed to be worn on the upper arm (Fig. 4b). The EMG signals of the antagonist's muscles are sensed by the textile sensors. Each muscle of extensor and flexor has two fabric-based electrodes to measure their muscle signal and there is one reference electrode to reduce the common mode noise. The electric contacts between the fabric-based sensor and the Bluetooth controller are achieved by metallic buttons.

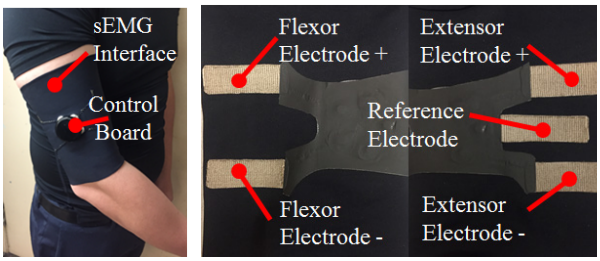

(a) (b)

Fig. 4. Configuration of wearable sEMG surface: (a) shows the wearable sEMG interface and its portable control board; (b) shows the designed wearable EMG sensors has five electrodes, two pairs of electrodes for measuring biceps and triceps muscle signal separately, another one electrode as a reference.

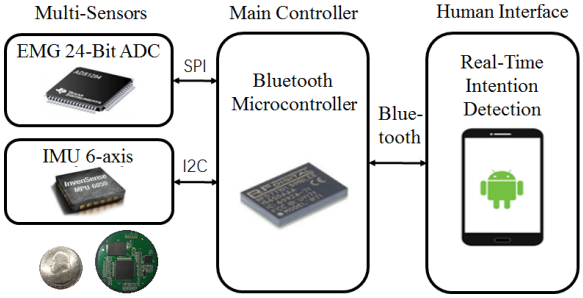

Fig. 5. The control system of the sEMG interface uses multi-sensors to detect human intention, it features low volume and low power consumption. The system uses Bluetooth Microcontroller (RFD77101, RF Digital, US) as the main controller to obtain and process the sEMG (ADS1294, Texas Instruments, US) and IMU (MPU6050, InvenSense, US) signal. Based on data fusion and identification, the system detects human motion intention and transmits the result to the human interface through the Bluetooth communication. Additionally, the results can also be used to control our design of a finger assistive and rehabilitation device.

The system board is composed of a 24-bit ADC ADS1294 (TI, Dallas, TX, USA), gyroscope & accelerometer MPU-6050 (InvenSense Inc., Sunnyvale, CA, USA), and a low-energy Bluetooth controller, as shown in Fig. 5. The muscle signals are acquired by the 24-bit ADC ADS1294 and the motion signals are acquired by the 16-bit 3-axial accelerometer and 3-axial gyroscope. Those EMG and motion data are collected by the controller and sent to a cell phone via Bluetooth.

D. Electronics Design

Because our design is for both SCI and stroke patients whose hand motor function is impaired, it is important to control finger flexion/extension in a simple way. After performing usability evaluations of different sensors, including bending sensor, inertial measurement unit (IMU) and electromyography (sEMG), we found that using only one of these sensors individually does not satisfy the need for detecting move intention of both SCI and stroke patients. We also found using data fusion of IMU and sEMG signal can enhance patients' finger movement intention detection effect to an acceptable level. Based on this, Fig. 6 shows the control system diagram using both IMU and sEMG to realize control feedback.

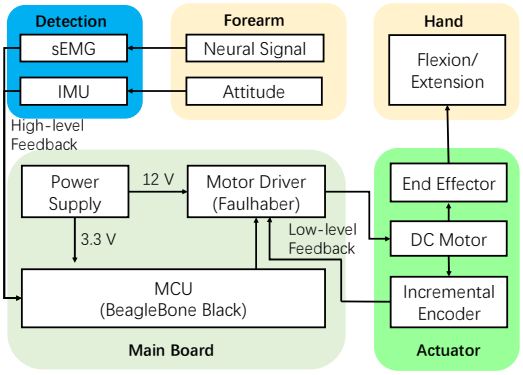

Fig. 6. The diagram shows the control system of the design. When patients want to flex/extend their finger, the neural and muscular properties of his/her arm will be slightly changed. The IMU and sEMG sensor can detect this variation and send signals to the microcontroller unit (MCU). Based on these feedback signals, the MCU processes the data and controls the DC motor, thus actuating the end-effectors to assist finger movement.

The electronics design mainly consists of the main control board, an actuator unit, and sensor boards. A commercially available MCU (BeagleBone Black development board, Texas Instruments LLC) is used with the main control board. The board handles IMU and sEMG data acquisition through UART communication, and handles sending motor control commands using PWM. Additionally, to develop the system quickly, a commercially available motor controller (MC5010S, Faulhaber LLC) located on the main board is used to implement low-level, closed-loop motor control. The actuator unit consists of a DC motor (12 V, 3.66W), gearbox (43:1 ratio, 3 stages planetary), and encoder (64 line, incremental). Two sensor boards are used to detect the patient's movement intention; one is a commercial attitude and heading reference system, which consists of a three-axis accelerometer, a three-axis gyroscope, and a three-axis magnetometer; another is a custom-designed sEMG detection suit, which will be introduced in the next section. The motor controller and DC motor are powered by 12 V DC supply and the MCU and sensor boards are powered by 3.3 V.

IV. EXPERIMENTS AND PERFORMANCE EVALUATION

Tests were performed twice on the actuator and once for the soft sEMG interface. The first test on the actuator measured the position control effect of the DC motor, and the second test attempted to determine the relationship between motor rotation and end-effector bending angle in different locations. The sEMG interface was then tested to determine if flexion/extension intention was detected by biceps and triceps sEMG signal variation. These tests verified the basic function of the actuator and soft sEMG interface prototypes.

A. *Low-Level Position Control Test*

The DC motor can actuate the end-effector through a cable-drive and assist finger flexion/extension. Based on the current version of the mechanical structure, the range of motion in the DC motor is from 0 to 130 degrees. 0 degrees corresponds to maximum extension state, and 130 degrees corresponds to maximum flexion state. A low-level position control loop was designed and run in the motor controller. Fig. 7 shows the result of the step signal test. The motor takes about 0.165 s to reach 130 degrees from 0 and about the same time to move back to 0 degrees again.

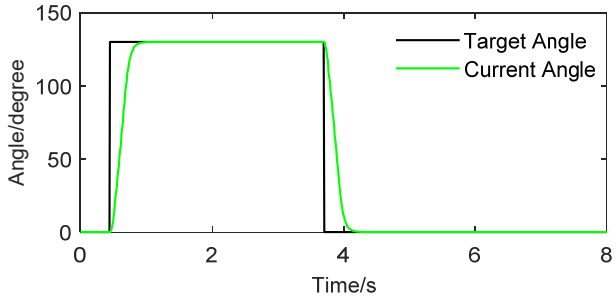

Fig. 7. DC motor low-level position control test. It shows the control result when motor rotate between 0 degrees (finger maximum extension) to 130 degrees (finger maximum flexion).

B. *End-effector Flexion/Extension Test*

The end-effector is fixed at the top of the finger and will assist finger flexion/extension through finger joints rotation. Due to the end-effector's soft design, unlike normal rigid structure, it's state of motion is hard to estimate. Thus, to assist the fingers flexion/extension movement, it is important to know the motion relationship between motor and end-effector. To measure finger joint rotation angles corresponding to DC motor position, an AHRS system (9-axis IMU sensor, HI219M, HiPNUC Technologies) has been used to measure the end-effector's rotation angle variation while the DC motor actuates from maximum extension to maximum flexion. As shown in Fig. 8(a), we put the AHRS system in six locations to test the end-effector rotation angle when it is actuated to assist finger flexion/extension.

A healthy 25-year-old man who is about 183cm high and weighs 80kg participated in this test. He wore the end-effector on his index finger. His hand was fixed in the same location throughout the entire test. The test repeats six times with the AHRS system fixed in different positions. During each test, the DC motor rotates from 0 degrees (maximum extension state) to 130 degrees (maximum flexion state) with a step of 13 degrees per second, rotating totally in 10 seconds. The AHRS system has a working frequency of 200 Hz. We use the average of 10 measurement data (0.05 s total) to indicate joint rotation variation at each second corresponding to DC motor position variation.

The result is shown in Fig. 8(b). With the DC motor rotating between 0 to 130 degrees, the change in shape of the end-effector and assist finger flexion/extension can be found. Between the finger maximum extension state and maximum flexion state, the finger dorsal side of each joint rotates 56.35 (MCP dorsal), 66.17 (PIP dorsal) and 101.74 (DIP dorsal) degrees, and the finger palmar side of each joint rotates 30.71 (MCP palmar), 75.64 (PIP palmar) and 109.11 (DIP palmar) degrees, separately. Although individual differences certainly exist, this experiment attempted to correspond the rotation position of the motor with the angle of the end-effector to assist the finger extension/flexion. This is helpful to guide us to control the whole system and demonstrate the effectiveness of the end-effector structural design introduced in this paper.

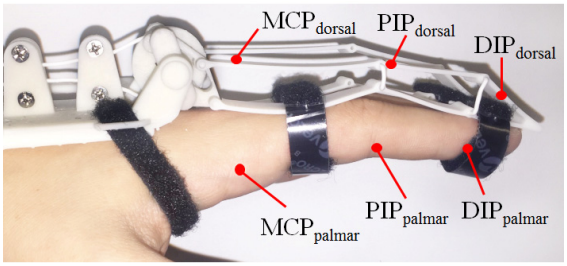

(a)

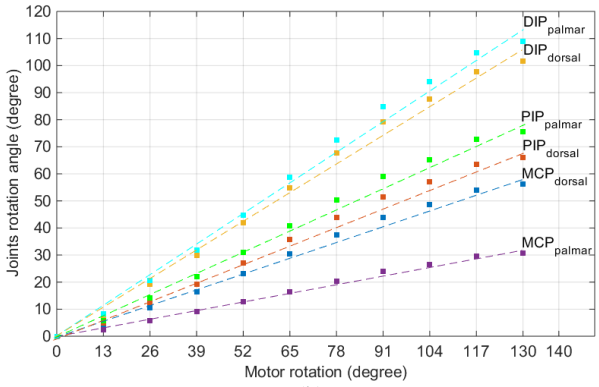

(b)

Fig. 8. Test of the end-effector flexion/extension range of motion with the DC motor rotating through 0 to 130 degrees. (a) shows the six IMU wearing fixed position, including three finger palmar side and three finger dorsal side of the actuator; (b) shows the result of testing parts' rotation variation correspond to the motor rotation between 0 (maximum extension state) to 130(maximum flexion state) degrees.

V. Conclusion

In this paper, we introduced a soft under-actuated hand exoskeleton which can facilitate both the rehabilitation and ADLs of stroke or SCI patients with paretic hand problems. Bio-inspired fin-ray grippers were adopted to provide patients with a soft and comfortable interface between their fingers and the exoskeleton. While simple and lightweight, our cable transmission system maintains steady and bidirectional assistance. The experimental results demonstrate the quick and accurate tracking performance of the low-level position control system.

References

[1] K. P. Westlake and N. N. Byl, "Neural plasticity and implications for hand rehabilitation after neurological insult," *J. Hand Ther.*, vol. 26, no. 2, pp. 87–93, 2013.

[2] A. Hogan, N.; Krebs, H.I.; Charnnarong, J.; Srikrishna, P.; Sharon, "MIT - MANUS : A Workstation for Manual Therapy and Training I," *MIT*, pp. 161–165, 1992.

[3] P. S. Lum, C. G. Burgar, M. Van der Loos, P. C. Shor, M. Majmundar, and R. Yap, "MIME robotic device for upper-limb neurorehabilitation in subacute stroke subjects: A follow-up study," *J. Rehabil. Res. Dev.*, vol. 43, no. 5, p. 631, 2006.

[4] P. Sale, V. Lombardi, and M. Franceschini, "Hand robotics rehabilitation: Feasibility and preliminary results of a robotic treatment in patients with hemiparesis," *Stroke Res. Treat.*, 2012.

[5] B. Kim and A. D. Deshpande, "Controls for the shoulder mechanism of an upper-body exoskeleton for promoting scapulohumeral rhythm," in *IEEE International Conference on Rehabilitation Robotics*, 2015, vol. 2015–Septe, pp. 538–542.

[6] D. Gijbels, I. Lamers, L. Kerkhofs, G. Alders, E. Knippenberg, and P. Feys, "The Armeo Spring as training tool to improve upper limb functionality in multiple sclerosis: a pilot study," *J. Neuroeng. Rehabil.*, vol. 8, no. 1, p. 5, 2011.

[7] P. Polygerinos, K. C. Galloway, E. Savage, M. Herman, K. O'Donnell, and C. J. Walsh, "Soft robotic glove for hand rehabilitation and task specific training," *Proc. - IEEE Int. Conf. Robot. Autom.*, vol. 2015–June, no. June, pp. 2913–2919, 2015.

[8] P. Polygerinos, Z. Wang, K. C. Galloway, R. J. Wood, and C. J. Walsh, "Soft robotic glove for combined assistance and at-home rehabilitation," *Rob. Auton. Syst.*, vol. 73, pp. 135–143, 2015.

[9] M. Nilsson, J. Ingvast, J. Wikander, and H. Von Holst, "The Soft Extra Muscle system for improving the grasping capability in neurological rehabilitation," *2012 IEEE-EMBS Conf. Biomed. Eng. Sci. IECBES 2012*, no. December, pp. 412–417, 2012.

[10] H. K. Yap, J. H. Lim, F. Nasrallah, J. C. H. Goh, and R. C. H. Yeow, "A soft exoskeleton for hand assistive and rehabilitation application using pneumatic actuators with variable stiffness," in *Proceedings - IEEE International Conference on Robotics and Automation*, 2015, vol. 2015–June, no. June, pp. 4967–4972.

[11] D. Park, I. Koo, and K. J. Cho, "Evaluation of an improved soft meal assistive exoskeleton with an adjustable weight-bearing system for people with disability," *IEEE Int. Conf. Rehabil. Robot.*, vol. 2015–Septe, pp. 79–84, 2015.

[12] H. In, B. B. Kang, M. K. Sin, and K. J. Cho, "Exo-Glove: A wearable robot for the hand with a soft tendon routing system," *IEEE Robot. Autom. Mag.*, vol. 22, no. 1, pp. 97–105, 2015.

[13] H. In, U. Jeong, H. Lee, and K. J. Cho, "A Novel Slack-Enabling Tendon Drive That Improves Efficiency, Size, and Safety in Soft Wearable Robots," *IEEE/ASME Trans. Mechatronics*, vol. 22, no. 1, pp. 59–70, 2017.

[14] U. Jeong, H. K. In, and K. J. Cho, "Implementation of various control algorithms for hand rehabilitation exercise using wearable robotic hand," *Intell. Serv. Robot.*, vol. 6, no. 4, pp. 181–189, 2013.

[15] B. B. Kang, H. Lee, H. In, U. Jeong, J. Chung, and K. Cho, "Development of a Polymer-Based Tendon-Driven Wearable Robotic Hand," pp. 3750–3755, 2016.

[16] B. Biorob, M. Xiloyannis, L. Cappello, D. B. Khanh, S. Yen, and L. Masia, "This document is downloaded from DR-NTU , Nanyang Technological University Library , Singapore . Modelling and Design of a Synergy-based Actuator for a Tendon-driven Soft Robotic Glove based Actuator for a Tendon-driven Soft Robotic Glove . Modelling and ," 2016.

[17] B. Radder *et al.*, "User-centred input for a wearable soft-robotic glove supporting hand function in daily life," *IEEE Int. Conf. Rehabil. Robot.*, vol. 2015–Septe, pp. 502–507, 2015.

[18] Z. B. Zhang, Y. H. Shen, W. D. Wang, B. Q. Wang, and J. W. Zheng, "Design and implementation of sensing shirt for ambulatory cardiopulmonary monitoring," *J. Med. Biol. Eng.*, vol. 31, no. 3, pp. 207–216, 2011.

[19] D. S. Nichols-Larsen, P. C. Clark, A. Zeringue, A. Greenspan, and S. Blanton, "Factors influencing stroke survivors' quality of life during subacute recovery," *Stroke*, vol. 36, no. 7, pp. 1480–1484, 2005.

[20] E. Weening-Dijksterhuis, M. H. de Greef, E. J. Scherder, J. P. Slaets, and C. P. van der Schans, "Frail institutionalized older persons: A comprehensive review on physical exercise, physical fitness, activities of daily living, and quality-of-life," *Am J Phys Med Rehabil*, vol. 90, no. 2, pp. 156–168, 2011.

[21] A. Cuppone, V. Squeri, M. Semprini, and J. Konczak, "Robot-assisted training to improve proprioception does benefit from added vibro-tactile feedback," in *Proceedings of the Annual International Conference of the IEEE Engineering in Medicine and Biology Society, EMBS*, 2015, vol. 2015–November, pp. 258–261.

[22] M. Stoppa and A. Chiolerio, "Wearable electronics and smart textiles: A critical review," *Sensors (Switzerland)*, vol. 14, no. 7. pp. 11957–11992, 2014.

[23] F. Axisa, P. M. Schmitt, C. Gehin, G. Delhomme, E. McAdams, and A. Dittmar, "Flexible technologies and smart clothing for citizen medicine, home healthcare, and disease prevention," *IEEE Trans. Inf. Technol. Biomed.*, vol. 9, no. 3, pp. 325–336, 2005.

[24] J. Wang, C. C. Lin, Y. S. Yu, and T. C. Yu, "Wireless Sensor-Based Smart-Clothing Platform for ECG Monitoring," *Comput. Math. Methods Med.*, vol. 2015, 2015.

[25] A. Shafti, R. B. Ribas Manero, A. M. Borg, K. Althoefer, and M. J. Howard, "Embroidered Electromyography: A Systematic Design Guide," *IEEE Trans. Neural Syst. Rehabil. Eng.*, vol. 25, no. 9, pp. 1472–1480, 2017.

[26] T. Finni, M. Hu, P. Kettunen, T. Vilavuo, and S. Cheng, "Measurement of EMG activity with textile electrodes embedded into clothing," *Physiol. Meas.*, vol. 28, no. 11, pp. 1405–1419, 2007.

[27] X. Tao, V. Koncar, T. H. Huang, C. L. Shen, Y. C. Ko, and G. T. Jou, "How to make reliable, washable, and wearable textronic devices," *Sensors (Switzerland)*, vol. 17, no. 4, 2017.

[28] C.-L. Shen *et al.*, "Respiratory Rate Estimation by Using ECG, Impedance, and Motion Sensing in Smart Clothing," *J. Med. Biol. Eng.*, vol. 37, no. 6, pp. 826–842, 2017.

[29] C.-L. SHEN *et al.*, "SMART EMG SLEEVE FOR MUSCLE TORQUE ESTIMATION," in *Uncertainty Modelling in Knowledge Engineering and Decision Making*, pp. 549–554.

[30] O. Pfaff, S. Simeonov, I. Cirovic, and P. Stano, "Application of Fin Ray effect approach for production process automation," *Ann. DAAAM 2011 Proc. 22nd Int. DAAAM Symp.*, vol. 22, no. 1, pp. 1247–1248, 2011.

[31] S. Alben, P. G. Madden, and G. V. Lauder, "The mechanics of active fin-shape control in ray-finned fishes," *J. R. Soc. Interface*, vol. 4, no. 13, pp. 243–256, 2007.

[32] A. Sunderland, D. Tinson, L. Bradley, and R. L. Hewer, "Arm function after stroke. An evaluation of grip strength as a measure of recovery and a prognostic indicator.," *J. Neurol. Neurosurg. Psychiatry*, vol. 52, no. 11, pp. 1267–1272, 1989.

[33] C. Bütefisch, H. Hummelsheim, P. Denzler, and K. H. Mauritz, "Repetitive training of isolated movements improves the outcome of motor rehabilitation of the centrally paretic hand," *J. Neurol. Sci.*, vol. 130, no. 1, pp. 59–68, 1995.

[34] M. A. Delph, S. A. Fischer, P. W. Gauthier, C. H. M. Luna, E. A. Clancy, and G. S. Fischer, "A soft robotic exomusculature glove with integrated sEMG sensing for hand rehabilitation," *IEEE Int. Conf. Rehabil. Robot.*, 2013.

[35] A. A. Timmermans, H. A. Seelen, R. D. Willmann, and H. Kingma, "Technology-assisted training of arm-hand skills in stroke: concepts on reacquisition of motor control and therapist guidelines for rehabilitation technology design," *J. Neuroeng. Rehabil.*, vol. 6, no. 1, p. 1, 2009.

[36] D. Jack *et al.*, "Virtual Reality-Enhanced Stroke Rehabilitation," vol. 9, no. 3, pp. 308–318, 2001.

[37] H. M. Hondori, M. Khademi, L. Dodakian, S. C. Cramer, and C. V. Lopes, "A spatial augmented reality rehab system for post-stroke hand rehabilitation," *Stud. Health Technol. Inform.*, vol. 184, pp. 279–285, 2013.

[38] The Mathworks Inc., "MATLAB - MathWorks," *www.mathworks.com/products/matlab*, 2016. .

[39] G. J. Snoek, M. J. Ijzerman, H. J. Hermens, D. Maxwell, and F. Biering-Sorensen, "Survey of the needs of patients with spinal cord injury: Impact and priority for improvement in hand function in tetraplegics," *Spinal Cord*, vol. 42, no. 9, pp. 526–532, 2004.